

# Comparison of Proximal Leg Strain in Locomotor Model Organisms Using Robotic Legs

Gesa F. Dinges , William P. Zyhowski , C. A. Goldsmith , and Nicholas S. Szczecinski (B)

Neuro-Mechanical Intelligence Laboratory, CEMR Mechanical and Aerospace L4, West Virginia University, Morgantown, WV, USA nicholas.szczecinski@mail.wvu.edu

**Abstract.** Insects use various sensory organs to monitor proprioceptive and exteroceptive information during walking. The measurement of forces in the exoskeleton is facilitated by campaniform sensilla (CS), which monitor resisted muscle forces through the detection of exoskeletal strains. CS are commonly found in leg segments arranged in fields, groups, or as single units. Most insects have the highest density of sensor locations on the trochanter, a proximal leg segment. CS are arranged homologously across species, suggesting comparable functions despite noted morphological differences. Furthermore, the trochanter-femur joint is mobile in some species and fused in others. To investigate how different morphological arrangements influence strain sensing in different insect species, we utilized two robotic models of the legs of the fruit fly Drosophila melanogaster and the stick insect Carausius morosus. Both insect species are past and present model organisms for unraveling aspects of motor control, thus providing extensive information on sensor morphology and, in-part, function. The robotic models were dynamically scaled to the legs of the insects, with strain gauges placed with correct orientations according to published data. Strains were detected during stepping on a treadmill, and the sensor locations and leg morphology played noticeable roles in the strains that were measured. Moreover, the sensor locations that were absent in one species relative to the other measured strains that were also being measured by the existing sensors. These findings contributed to our understanding of load sensing in animal locomotion and the relevance of sensory organ morphology in motor control.

Keywords: Strain  $\cdot$  Campaniform sensilla  $\cdot$  Load  $\cdot$  Walking  $\cdot$  Insect

# 1 Introduction

The ability to monitor and respond to dynamic, mechanical stimuli is an important aspect of robust locomotion. Multiple sensory structures sensitive to proprioceptive stimuli can be found in insect legs (Fig. 1A). Their collective output can be integrated

G. F. Dinges and W. P. Zyhowski—These authors contributed equally to this work.

<sup>©</sup> The Author(s), under exclusive license to Springer Nature Switzerland AG 2023 F. Meder et al. (Eds.): Living Machines 2023, LNAI 14157, pp. 411–427, 2023.

in the nervous system to modify or reinforce motor output, contributing to adaptability. Sensing the magnitudes and dynamics of forces that arise during walking provides useful information to the locomotor system [1, 2]. Changes in force that each leg experiences are accompanied by changes in load. Because the gravitational load that the body exerts on the legs must be continuously supported [3], the measurement of forces in the legs can influence individual legs to transition between their stance and swing phases during walking [4], ultimately influencing interleg coordination [5, 6].

Campaniform sensilla (CS) are sensory organs that facilitate force measurements, monitoring resisted muscle forces through the detection of strains in the exoskeleton [7, 8] (Fig. 1A1). Resisted muscle forces arise as legs transition during stepping from the swing to the stance phase, during which body weight support is initialized. CS are embedded within the exoskeleton, with cap-like structures that deform when the surrounding cuticle is strained. Electrophysiological experiments have shown that CS fire during the onset of the anterior extreme position (anterior-most position at the onset of stance phase, AEP) [8, 9] (Fig. 1A2). This type of CS activity can enhance the magnitude of muscular contractions, increasing support for the added load [7, 10, 11]. CS also signal the termination of the stance phase at the posterior extreme position (posterior-most position at the termination of stance phase, PEP) [6, 12] (Fig. 1A2). Between the onset and termination of stance phase, the neuronal responses of CS adapt under exposure to force [2, 13].

Leg CS are generally located in the proximity of joints [14]. There, they can be found in fields, groups, or as single sensors [15–18]. In groups and fields, CS caps are commonly elliptical, with the orientation of their axes producing directional sensitivity [8, 13, 14, 19–21]. This is beneficial for two reasons, as multiple sensors with the same orientation allow for range fractionation in force encoding and redundant measurements reduce noise [1, 22]. Moreover, different components of forces can be measured depending on the orientation of a sensor relative to limb segments. For example, axial torques, as seen during supination and pronation movements, create helical forces that can be detected by sensors with a long-axis orientation of 45° relative to the limb's long axis [6, 13].

Groups and fields of CS are more commonly found in proximal leg segments [23]. The trochanter, a limb segment located between the coxa, the most proximal limb segment, and femur, the limb-segment between trochanter and tarsus, acts as a focal point for forces generated by multiple leg and body muscles [24, 25]. In the stick insect Carausius morosus, four fields of CS on the posterior, anterior, and dorsal faces encode external loads and strains [25, 26]. Within each field, the sensors' long-axis orientations are similar, creating functional subunits [26]. Extensive electrophysiological investigations in C. morosus have shown that groups G1 and G2 on the posterior and anterior trochanter monitor load in the posterior and anterior direction, respectively [19, 26, 27]. G3, on the dorsal trochanter, encodes increases in dorsal load and decreases in ventral load [25], while G4, also on the dorsal trochanter, shows mirrored directional sensitivities and directly responds to depressor muscle contractions [25]. Together, G3 and G4 encode the increases and decreases of load in the dorsal-ventral plane of the coxa-trochanter joint [25].

Other insects, even the significantly smaller and lighter fruit fly *Drosophila melanogaster*, have CS in some of the same leg locations, indicating potential functional homology; however, morphological differences have been noted [1, 17, 28]. The *D. melanogaster* trochanter contains the trochanter field (TrF), which is homologous to G3 + G4 and consists of two subunits [15, 17, 18]. Further, a group of three sensors can be found on the posterior trochanter, all with the same axis orientations. Unlike in *C. morosus* and the cockroach *Periplaneta americana*, *D. melanogaster* and the blow fly *Calliphora vomitoria* do not have anterior trochanteral CS [1].

Although both species have CS on their trochanter, the trochanter–femur joints' mobility may influence strain sensing in these locations. This joint in *C. morosus* is fused [29–31], while in *D. melanogaster* the joint's mobility has not been conclusively determined [32–35]. Changing the mobility of this joint may contribute to changes in the orientation of the leg, impacting force distributions across the various leg segments. In this manner, leg orientation has been found to directly affect CS discharge [25]. Although the principal aspects of locomotion are comparable between different insects, characteristics such as body weight, leg and sensor morphology, and average walking speed may influence the activity of leg CS. Body weight has been shown to be reflected in the range of cap sizes [1] as well as the number of CS. *C. morosus*, with an average mass of 800 mg, has more CS than the 1-mg *D. melanogaster*. However, the 30-mg juvenile cockroach contains a similar number of CS as *D. melanogaster*. This suggests that the fly's CS fields may monitor the same force despite the insect's size [1]. Nonetheless, flies are significantly smaller than the insects that have commonly been used to study leg CS function, which introduces methodological limitations.

A key element for investigating the function of load sensors within neuromuscular systems is understanding what strains arise in different limb segments during cyclic movements. While larger insects like cockroaches and stick insects allow for the direct measurement of strains [36] and neuronal activity [6, 13, 19, 23, 25, 26, 28, 37, 38], smaller insects like *D. melanogaster*, while advantageous because of its vast genetic toolbox, only produce minute forces that are difficult to monitor using modern tools. Thus, approaches like that of Zyhowski et al. (2023), which used a stick insect-inspired robotic leg to analyze strain patterns similarly to electrophysiological experiments in real animals, provide an opportunity to investigate strain in smaller insects.

In the present study, we utilized an updated robotic leg modeled from *D. melanogaster* [39] and a robotic leg modeled from *C. morosus* [40], with both legs dynamically scaled to each insect. These legs should experience inertial, viscous, elastic, and gravitational forces proportionally similar to the corresponding insect legs. We investigated what strains are detected by sensors with correct orientations and what is detected by the fields that are present in some species and absent in others. The results underlined that the sensor locations and leg morphology influenced the detected strains in the proximal leg segment, creating noticeable differences in which aspects of load changes throughout the stance phase were captured. Further, the "missing" sensor locations detected tensile strains similar to those detected by sensors in existing locations on the other animal. These findings aid our understanding of load sensing and the relevance of sensory organ morphology.

# 2 Materials and Methods

## 2.1 General Setup

Based on previous publications [39, 40], the legs consisted of three MX-28AT Dynamixel servomotors (Dynamixel, Seoul, Korea) connected in series via brackets and hollow 3D-printed limb segments manufactured with Onyx [41] using a Markforged Mark 2 (Markforged, Waltham, MA, USA). MATLAB (2021b; MathWorks, Natick, MA, USA) controlled the servomotor angles to execute footpaths based on the inverse kinematics published in Zyhowski et al. (2023; Fig. 1 B, C). For the *D. melanogaster* model, the inverse kinematics were calculated in the same manner; however, a shorter step trajectory was implemented based on published data [34]. Consequently, the legs stepped on a treadmill (as in Zyhowski et al., 2023), simulating an anteriorly directed body movement similar to those seen in walking animals. During the stance phase in each step, the leg supported the carriage's weight and simulated body weight using a linear guide (Fig. 1). To simulate different walking speeds, we altered the duration of the stance phase: (1) 2-s swing, 2-s stance; (2) 2-s swing, 4-s stance; and (3) 2-s swing, 6-s stance.

Strains were detected using strain gauge rosettes (C5K-06-S5198–350-33F; Micro-Measurements, Raleigh, NC, USA). Using operational amplifiers, their signals were amplified and converted to 12-bit digital signals using an OpenCM 9.04 microcontroller (Robotis Inc., Lake Forest, CA, USA). Strain gauges were placed onto the proximal-most end of the femur in each leg based on published scanning electron images of *C. morosus* [42] and *D. melanogaster* [15] (Fig. 1 Bi-B3, Ci-C3). Because CS are most sensitive to strains along their short axis, we oriented the strain gauges to match the short axis orientations of the majority of the CS within each location [8, 13, 14, 20, 21, 43] (Fig. 1A2). This also determined our labeling of each location, with *axial* describing the group with more short axes along the axial plane of the leg, and *transverse* the group with more short axes along the transverse axes of the leg. For locations with CS that have mirrored axes (G2, G3 + 4, TrF) we used two of the strain gauge axes, set perpendicular to each other by 90°, to capture the naturally occurring sensitivities of the CS fields. For the locations without a perpendicular subgroup (G1, TrG), we also recorded from two strain gauge axes to measure any strains that the animals do not capture (Fig. 1 B3, C3).

# 2.2 Legs

To compare how different leg morphologies may contribute to different proximal strains, we used two different robotic legs, one for each insect (Fig. 1 B1-B2, C1-C1). For the stick insect, we used a scale of 25:1, which is an upscaled version of the Zyhowski et al. (2023) leg. For the fly, we used an updated version of the Goldsmith et al. (2019) Drosophibot leg, scaled 400:1. By scaling the legs in this manner, both robotic legs had the same length dimensions.

In addition to scaling, the stick insect leg was further modified by adding a round, silicone foot. In preliminary experiments, this increased friction with the substrate, which prevented the leg from slipping on the treadmill. These types of friction-increasing components are common in insects such as the adhesive organs found on the *C. morosus* tarsus [44]. The same foot was also attached to the *Drosophila* leg (Fig. 1A1).

Figure 1B1 shows the robotic stick insect leg, which had 3 degrees of freedom and was modeled after the morphology detailed in Cruse et al. (1995). The leg consisted of the coxa, a fused trochanter–femur, and tibia (limb-segment between femur and tarsus) segments. The movement of the leg was generated by the thorax–coxa (ThC,  $\vartheta_1$ ), coxa–trochanter (CTr,  $\vartheta_2$ ), and femur–tibia (FTi,  $\vartheta_3$ ) joints. Figure 1C1 shows the robotic fly leg, which also had 3 degrees of freedom and was modeled in a similar fashion based on the design from Goldsmith et al. (2019, 2022). It is important to note that both legs had the same degrees of freedom but differed in their axes of rotation (how the movement is generated). Specifically, the ThC and CTr joints rotated the legs in different planes. The FTi joint had the same axis of rotation in both robotic legs.

# 2.3 Dynamic Scaling

Because the robot legs are much larger and more massive than insect legs, it is necessary to dynamically scale their motion relative to that of the insects. Elastic and viscous forces have been shown to dominate the dynamics of insect leg joints [45–47], with legs possessing gravity-independent posture that slowly returns to equilibrium when disturbed. In contrast, robot legs (in particular, servomotors) are massive, meaning that even moderate accelerations during motion may result in large inertial forces. Furthermore, when powered down, robot legs hang with gravity, in stark contrast to insect legs [46]. These differences in dynamics were accounted for here in two ways. First, when the robot leg was powered up, the servomotors at their joints had programmed equilibrium angles and produced torque proportional to the deviation from these equilibrium angles, functioning like springs and imbuing the leg with an "active" elasticity. Powered up legs no longer hanged with gravity. Second, increasing the stepping period of the robot reduced leg acceleration and, therefore, inertial forces. The resulting robot legs exhibited a balance of inertial, viscous, elastic, and gravitational forces comparable to an insect, despite the magnitude of these forces being much larger in the robot legs.

We scaled the stepping period of the robotic legs by maintaining the same ratio between the motion's frequency and the leg's natural frequency (which depends on the balance between it elastic and inertial forces) in the robot and the insect. For example, *C. morosus* has an approximate natural period of 0.132 s [40] and a step period of around 1 s [48]; a step is approximately six times longer than the natural period. The robotic *C. morosus* leg was similar in that its natural period was 0.63 s [40], with a step period of approximately 4 s. The robotic *D. melanogaster* step time was calculated with the same process, and its step period was also approximately 4 s [34, 39].

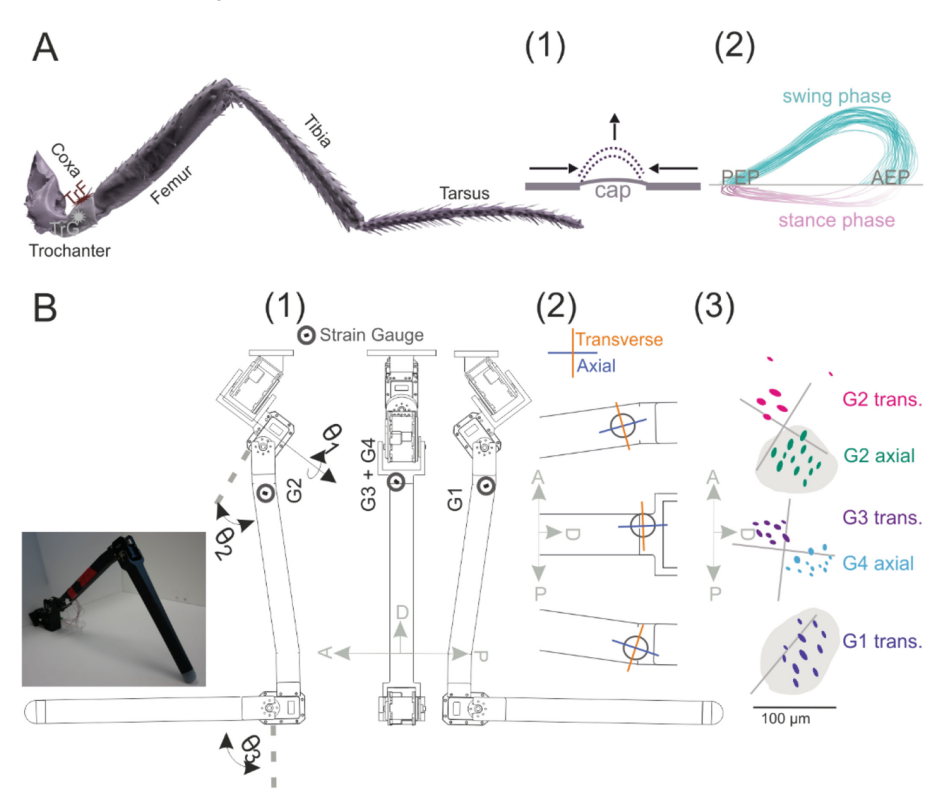


Fig. 1. Experimental Setup; (A) nano-CT rendered leg of *Drosophila melanogaster*. Image taken from Dinges et al., 2022, modified in color. Limb segment labels were added; TrF and TrG approximate locations were labeled; (A1) schematic drawing of a CS experiencing compressive strains, schematic cap undergoes lateral displacement; (A2) example trajectories of a *Drosophila* front leg step cycle. The trajectories were traced from tracked leg movements courtesy of the Büschges Lab (University of Cologne). PEP – posterior extreme position, AEP – anterior extreme position; (B) image of robotic stick insect leg; (B1) location of strain gauges on robotic stick insect leg; (B2) close up of B1, indicating axis orientations of strain gauges; joint angles are noted on the anterior face of the leg (B3) schematic drawing of CS morphology taken from published SEM images; gray circles indicate indentations in the cuticle; crosshairs display perpendicular compression axes at each location (C) image of robotic *Drosophila melanogaster* leg; (C1) location of strain gauges on robotic *D. melanogaster* leg; (C2) close up of B1, indicating axis orientations of strain gauges; joint angles are noted on the anterior and dorsal faces; (C3) schematic drawing of CS morphology taken from published SEM images; trans, transverse; both axial and transverse are relative descriptors. A, anterior face; D, dorsal face; P, posterior face.

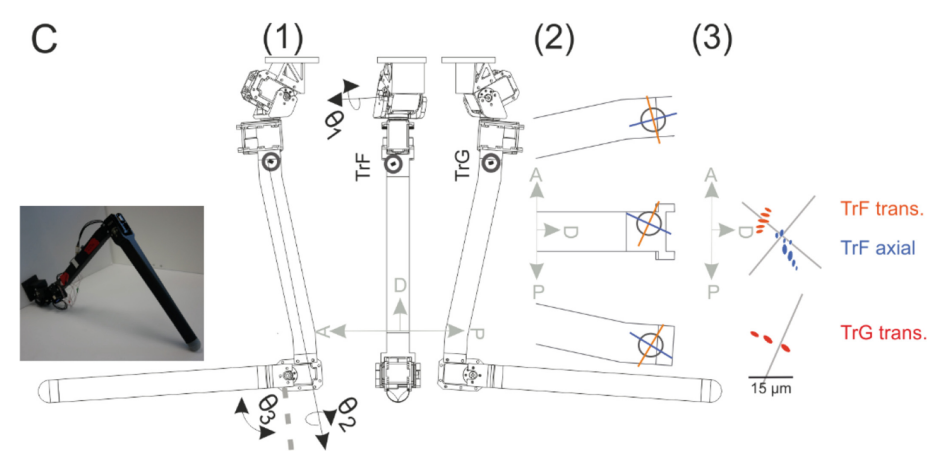


Fig. 1. (continued)

### 2.4 Data Analysis

Strain was detected over the course of 10 steps and averaged. The rate of change was calculated using averaged and smoothed strain data. All analyses were completed using MATLAB. Images were compiled using CorelDRAW (X8; Alludo, Ottawa, Canada).

# 3 Results

To investigate how insect leg morphology, stepping speed, and sensor presence and location affect strain monitoring during walking, we evaluated the strains that stick insect- and *Drosophila*-like robotic leg segments experience during treadmill stepping.

# 3.1 Strains Detected by CS-Like Sensors

To test how changes in stepping speed affect strain monitoring in the legs, we recorded strain during stepping on a treadmill at three different speeds. The speeds were modulated by altering the duration of the stance phase (2 s/4 s/6 s), ultimately prolonging the duration for which the leg was required to support the "body".

The two strain locations on the anterior face of the leg, G2 transverse and G2 axial, detected different strains during the stance period. G2 transverse contains 6 CS and G2 axial contains 12 CS in the stick insect, and the CS of each subfield share the same short-axis orientations, with the two groups perpendicular to each other (Fig. 1 B3). In the robotic leg, G2 transverse detected decreases in strain, peaking at the AEP of the stance phase, indicating tensile strain. The detected strains decreased gradually over time after the AEP, with a small peak at the PEP. The rate of change in strain reached its lowest value at the AEP and its highest at the PEP (Fig. 2B). The G2 axial group was exposed to the inverse during stepping (Fig. 2A). Unlike G2 transverse, this location was under compressive force during the stance phase. At the AEP, a gradual increase in detected

strain began, which peaked at the PEP. The rate of change in strain increased slightly at the AEP, while it showed the greatest decrease at the PEP (Fig. 2B).

On the dorsal leg face, the more transverse G3 and the more axial G4 (Fig. 1B3), detected tensile strain with peaks in intensity at different times in the stance phase. In the animal, G3 contains 8 CS and G4 12 CS, with both locations showing similar short-axis orientations. G3 in the model, similarly to G2 axial, began monitoring strain at the AEP with the gradual increase in strain peaking at the PEP. This location experienced compressive force during the stance phase, with the greatest compression at the PEP. The rate of change in strain showed a positive peak at the AEP and a negative peak at the PEP. G4 also experienced compressive strains during the stance phase. However, unlike G3, it was exposed to the greatest amount of strain during the AEP rather than the PEP. Following this AEP peak, there was a gradual decrease in strain, with a further, smaller increase at the PEP. Similarly to G3, there was a positive rate of change at the AEP, followed by a negative peak at the PEP.

G1 is located on the posterior leg face in *C. morosus* and consists of 11 CS, which are largely oriented in the transverse direction (Fig. B3). Here, during stepping, G1 detected strain similarly to G4, with a primary peak at the AEP, followed by a gradual decline and a smaller peak at the PEP. It was also under compressive force during the stance phase. The rate of change in strain followed the same pattern as those of G2 axial, G3, and G4, with a positive peak at the AEP and negative peak at the PEP.

In the fly model, the anterior leg face contained no CS (Fig. 1C3); the CS closest to the anterior face (TrF transverse) detected tensile strain with a peak at the AEP. In the animal, this location contains five CS, all with the same short-axis orientation. This sensor location detected a rapid increase in strain with peak values at the AEP. The strain gradually decreased for the rest of the stance phase without a further increase at the PEP. The rate of change in strain only showed a positive peak at the AEP. This location was under compressive force during the stance phase. The more posterior subfield of the TrF, here referred to as TrF axial, contains 8 CS in the animal, all with the same short-axis orientation (Fig. 1C3). Similarly to TrF transverse, this location detected the greatest amount of strain at the AEP in our model; however, it detected tensile and not compressive forces. There was also a gradual decrease in strain through the rest of stance, with no further peaks. The rate of change in strain only showed a negative peak at the AEP.

The only remaining CS location of the fly, TrG, detected compressive strain. In the animal, it consists of three CS, all with the same short-axis orientation (Fig. 1C3). Similarly to TrF transverse, this location in our model experienced compressive forces and detected rapid increases in strain, peaking at the AEP. There was no further peak in strain measurement for the rest of the stance phase. Consequently, the rate of change in strain only increased at the AEP.

For all locations, independent of the modeled species, there were no apparent differences in the detected strains at different stepping speeds (Fig. 2A). This suggests that inertial forces do not dominate the dynamics and that the dynamic scaling of the leg was successful.

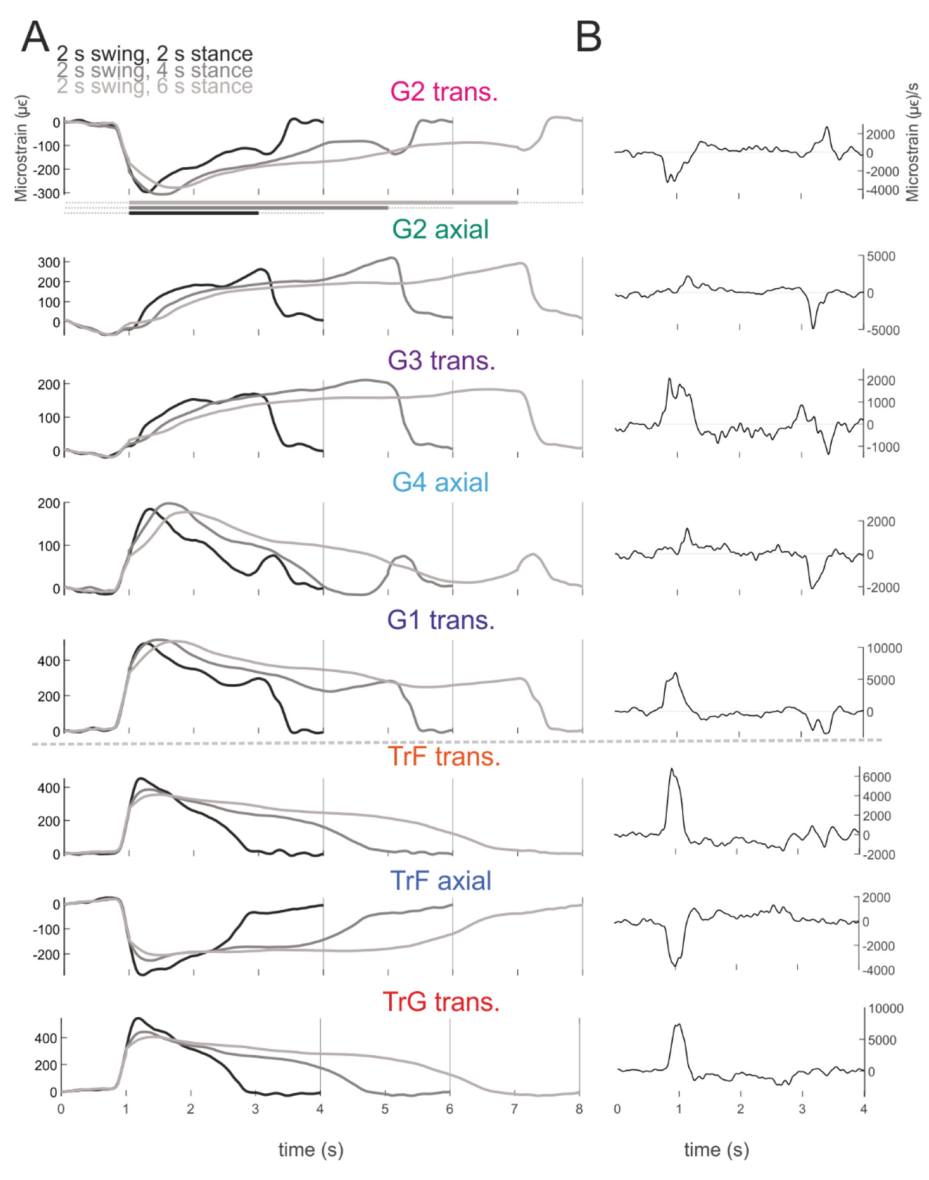


**Fig. 2. Strain during stepping at different speeds; (A)** strain recordings (microstrain) of the robotic stick insect (G2/G3/G4/G1) and *D. melanogaster* (TrF/TrG) at different stepping speeds; black line, 2 s swing, 2 s stance; grey, 2 s swing, 4 s stance; light grey, 2 s swing, 6 s stance; (**B)** rate of change (microstrain per s) curves for the 2-s swing/2-s stance strain recordings; trans, transverse; both axial and transverse are relative descriptors. Lines under plot G2 trans., schematize the swing phase using dotted lines, and stance phase using the solid line for each tested speed.

### 3.2 Undetected Strains

To test what would be measured by subfields and CS locations that exist in some species but not others, we detected strain in both axes of existing subfields as well as in artificial sensor locations. For the stick insect, this included the subfield perpendicular to the posterior transverse sensors, referred to as posterior axial (Fig. 1B2). For the fly, the added locations were on the anterior face and mirrored relative to those on the posterior face. These locations are referred to here as anterior transverse and anterior axial (Fig. 1C2). Further, a sensor perpendicular to the posterior transverse location was used, referred to here as posterior axial (Fig. 1C2). The experiments were completed using a step period of 2-s swing and 2-s stance phases.

In the stick insect, the only sensor location that does not have two subgroups is that of the posterior face, where the axial orientation is non-occurring (Fig. 3A). The strain that this sensor monitored was relatively consistent throughout the stance, with a peak at the PEP. This location was under tensile force during the stance phase, suggesting that it would not generate tonic sensory discharges during walking. The measurements at this location mirrored those of G3, which was under compressive force during the stance phase.

In the fly model leg, we used three artificial locations (Fig. 3B). A strain gauge mounted on the limb's anterior face mirrored the orientation of the strain gauge normally found on the posterior face. Additionally, the perpendicular axis of the posterior transverse strain gauge was also used as its artificial subgroup. All three artificial locations were under tensile displacement during the stance phase. Furthermore, the measured strains at all locations peaked at the AEP, similarly to the fly model. Both the posterior axial and anterior transverse groups mimicked the strains measured at TrF axial. The anterior axial also showed a similar response. Furthermore, this location seemed to monitor minor compressive forces at the PEP.

While the anterior CS locations are seen in the stick insect but not the fly, the artificial anterior transverse location detected the same strain as the stick insect's anterior transverse field (G2; Fig. 3). However, the artificial anterior axial sensor in the fly did not monitor the same strain as the stick insect anterior axial sensor (G2 axial). In the fly, this location experienced compressive force, while it experienced tensile force in the stick insect. Additionally, the fly anterior axial experienced the greatest strain at the AEP, while the stick insect anterior axial did so at the PEP.

The artificially placed posterior axial sensors, which do not exist in either animal, were under tensile force during the stance phase. However, this location was under the greatest strain at the PEP in the stick insect, while it experienced the greatest strain at the AEP in the fly.

### 4 Discussion

We compared changes in strain during stepping in two robotic legs, which were modeled after the morphology of two motor control model organism, *C. morosus* and *D. melanogaster*. We believe comparative studies not only benefit our understanding of proprioceptive function but also how species-specific morphology can affect homologous organs. The strains detected by the strain gauges reflected the onset of the AEP

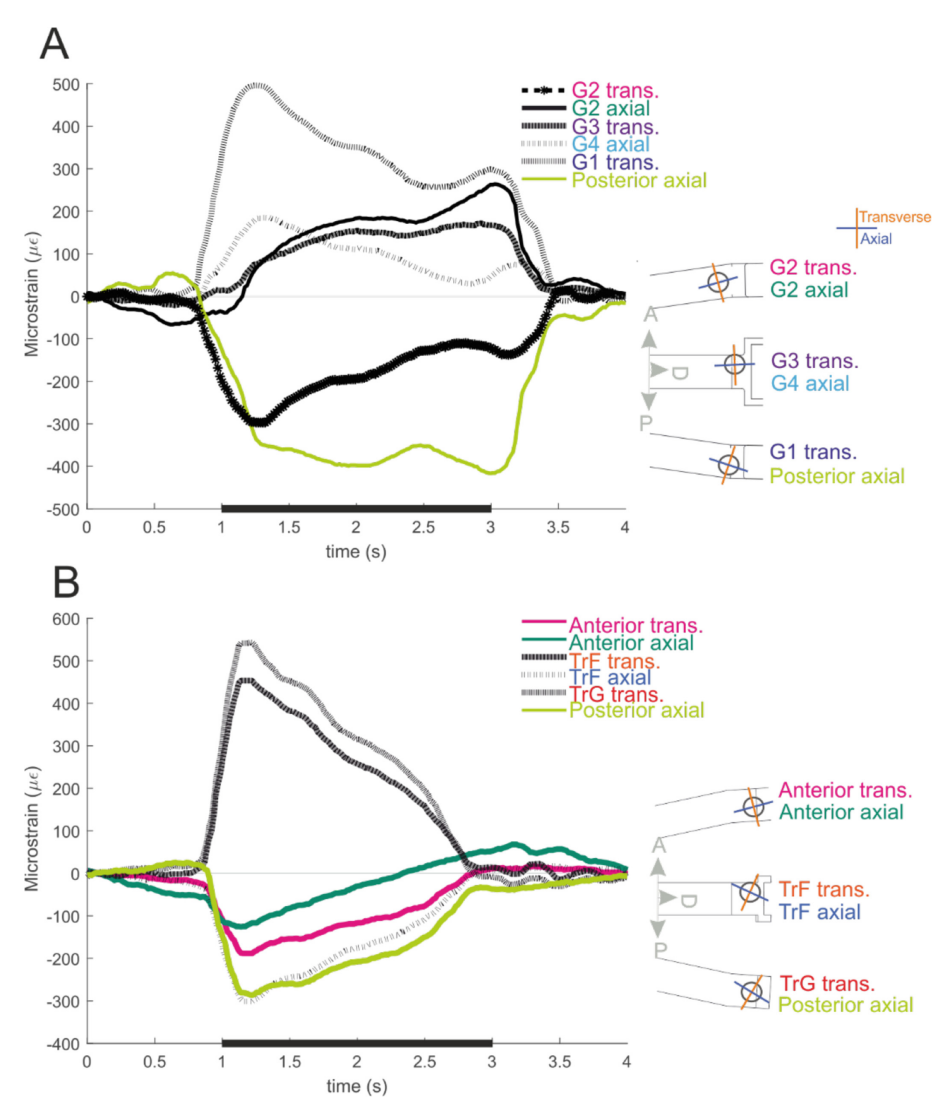


**Fig. 3.** All sensors on the robotic leg; (A) strain recordings of all strain gauges placed on the robotic stick insect leg; (B) strain recordings of all strain gauges placed on the robotic *D. melanogaster* leg; black lines mark proximal CS, colored lines mark artificially placed strain gauges; trans, transverse; both axial and transverse are relative descriptors. Bar along x-axes marks stance phase.

in both robotic legs. However, only the robotic leg model of *C. morosus* had sensors in locations predominantly sensitive to strains arising at the PEP, which is similar to results from electrophysiological recordings of all four stick insect trochanteral fields [25].

The stick insect G2 transverse, G4, and G1 transverse registered strain peaks at the AEP, while G2 axial and G3 peaked at the PEP. In the *D. melanogaster* model, TrF

transverse, TrF axial, and TrG all peaked at the AEP, with no further peaks at the PEP. This suggests that different trochanteral CS locations monitor different phases of the stance phase in the stick insect, while *D. melanogaster* trochanteral CS predominantly monitor the onset of stance. Additionally, in the stick insect leg model, the strain detected between the AEP and PEP was reflected in the course of sensor activity, which showed similarities between neighboring locations (Fig. 2A). The most anterior location (G2 transverse) detected peak tensile force at the AEP. Its subfield, G2 axial, detected compression at the PEP, as did its dorsal neighboring field, G3 transverse. G3 transverse's subfield, G4 axial, detected compressive strain at the AEP, and its posterior neighboring field, G1 transverse, detected the same compressive strain at the AEP. Similar to G2 transverse, the artificially placed G1 axial experienced tensile force, but showed different dynamics, with an extreme at the PEP (Fig. 3A). This pattern of strain monitoring suggests a phase shift-like progression in field activity, with two neighboring fields monitoring the same strains in a posterior-to-anterior tracking of the AEP to the PEP.

Unlike the stick insect model, in the robotic fly leg, all sensor locations registered the greatest strain at the AEP (Fig. 2A), including the artificial locations (Fig. 3B). These fundamental differences may be influenced by differences in body size. For example, in investigations of wing CS, the CS of larger insects with lower wingbeat frequencies functioned as magnitude detectors, while the CS of smaller insects with higher wingbeat frequencies only fired at single instances within the wing stroke [49]. In this way, sensors in larger insects primarily detected force magnitude, while those in smaller insects primarily detected timing. Similar to the shorter wingbeat periods, the faster average stepping in *D. melanogaster* compared to *C. morosus* may also reduce their tempo-ral integration capacity and, thus, enforce a reduction in monitoring of stance phase initiation [48–51].

Another possible explanation for the observed differences in load variation between species is the unique posture of the legs, in particular, how each leg is extended and supinated throughout stance. In general, extending the leg increases the moment arm of ground reaction forces at the foot, which should increase stress (and thus strain) on the proximal parts of the leg. Furthermore, because strain gauges (and CS) are directionally sensitive, pronating and supinating the leg will misalign the strain gauges from the axes of the predominant stresses. Because each animal's stepping motion is unique, these effects combine differently in each. Furthermore, our study was limited by the accessibility of the *D. melanogaster* robotic trochanter. We placed the trochanteral CS on the femur of both legs, which further changed their orientation throughout the step. In future investigations, we will extend the robotic *Drosophila* trochanter to fit the necessary CS and further explore the impact of the mobile trochanter—femur joint on load sensing.

For the stick insect, the leg extends to reach the AEP, flexes throughout the first half of stance, then extends throughout the second half of stance to reach the PEP [42]. As a result, the lever arm of the ground reaction force on the body starts large, then decreases, then increases. Simultaneously, the plane of the leg begins pronated and supinates throughout stance, meaning that stresses are initially not aligned with G4 axial, then align with G4 axial mid-stance, and finally misalign at the end of stance. These mechanisms appear to counterbalance one another, resulting in a relatively constant but ultimately "dual-peaked" profile in the stick insect G4 axial recording.

In contrast, the fruit fly leg remains quite flexed when reaching the AEP and then extends throughout stance to reach the PEP. Furthermore, the leg is neither pronated nor supinated at the AEP and is supinated at the PEP. These monotonic progressions from flexion to extension and from neutral to supination do not produce the same "dual-peaked" strain profiles seen in the stick insect. Instead, all the recordings from the fruit fly are "single-peaked". Although both species' legs perform the same roles of supporting and propelling the body, these differences in posture would certainly change the way that stress is applied to and resisted throughout the leg. Such postures may be the result of locomotion speed differences, as discussed above. An evolutionary and developmental survey of insect species, their locomotion speeds, their leg posture, and CS placement may reveal broader correlations between these behavioral and morphological properties.

The rate of change in strain at each sensor location may reflect neuronal activity during walking. CS discharges reflect both the amplitude and the rate of change of strain [2]. The aforementioned differences between the legs further suggest that the stick insect sensor locations monitor strain throughout the stance phase while those of *D. melanogaster* monitor strain solely at phase onset. Future investigations should model sensory discharges in response to the strain signals we recorded to gain insight into the features of loading that are emphasized within the nervous system. Potential experiments (i.e., using optogenetics) could illuminate if CS in *Drosophila* are active during the complete stance phase, during phases in which the rate of force changes, or solely at the onset of stance, as our experiments suggest.

The differences between the two legs in the functionality of the sensor locations legs, as discussed above, may also explain why *Drosophila* has fewer CS locations on its trochanter and the stick insect does not possess a G1 subfield. The *D. melanogaster* model's axial trochanter field detected tensile force at the AEP, which is what the missing locations would also monitor in this setup. The stick insect model's G3 transverse was under compression during the stance phase and detected similar strain developments as the missing posterior axial subfield. Additionally, all "missing" locations were exposed to tensile strain during stance phase, which may not lead to CS activity [43]. Notably, the present study was limited by the simplification of the sensor field by using strain gauges. The exact orientations of the caps within each field may vary, which could lead to sensory activation in individual sensors at different time points. Moreover, there may be differences in cellular properties between neurons associated with larger and smaller caps within one location.

In future studies, this experimental technique could be used to predict which CS fields and groups other insect species possess, based on the species' leg orientation and walking kinematics. Accurate predictions would support our main hypothesis that CS fields and groups that redundantly signal loads disappear over the course of evolution. Inaccurate predictions would suggest that this hypothesis is incomplete or incorrect. More closely examining the behavior of individual species may suggest other reasons for CS fields and groups changing over evolutionary time.

The present study investigated strains in a proximal limb segment in two morphologically different robotic legs. Generally, tension and compression were seen in the proximal limb segment of both robotic legs with amplitudes independent of the stepping

speed. Furthermore, the waveform of the strain did not change with stepping speed, indicating that inertial forces were not dominating, and that the robotic models mimicked the dynamics of insect locomotion. In both legs, all but one of the morphologically correct locations were positioned in locations that are sensitive to compressive strains during the stance phase. There are, however, key differences, including the monitoring of both the AEP and PEP in the stick insect model and only the AEP in D. melanogaster. Further, there were clear differences between the models in the amplitudes of the rates of change of strain, with single peaks in the fly and dual peaks in the stick insect. These differences may be due to joint angles, loads, or CS morphology and orientation. To investigate this further, future experiments should analyze how joint movements may influence strain sensing and apply a dynamic discharge model to the recorded strain to understand how different sensors in different organisms may physiologically respond to load. These results can be taken into account in future animal experiments, as understanding how extremity morphology contributes to mechanosensory activity eases knowledge transfer between species. In conclusion, the current work contributes to the understanding of how differences in load sensors may influence neuromuscular systems and motor control.

**Funding.** G.F.D., W.P.Z., C.A.G., and N.S.S. were supported by NSF DBI 2015317 as part of the NSF/CIHR/DFG/FRQ/UKRI-MRC Next Generation Networks for Neuroscience Program. W.P.Z. and N.S.S. were supported by NSF IIS 2113028. G.F.D. was supported by DFG DI 2907/1-1 (Project number 500615768).

# References

- Harris, C.M., Dinges, G.F., Haberkorn, A., Gebehart, C., Büschges, A., Zill, S.N.: Gradients in mechanotransduction of force and body weight in insects. Arthropod Struct. Dev. 58, 100970 (2020). https://doi.org/10.1016/j.asd.2020.100970
- Zill, S.N., Dallmann, C.J., Büschges, A., Chaudhry, S., Schmitz, J.: Force dynamics and synergist muscle activation in stick insects: the effects of using joint torques as mechanical stimuli. J. Neurophysiol. 120, 1807–1823 (2018). https://doi.org/10.1152/jn.00371.2018
- 3. Cruse, H.: Which parameters control the leg movement of a walking insect?: Ii. The start of the swing phase. J. Exp. Biol. 116, 357–362 (1985). https://doi.org/10.1242/jeb.116.1.357
- Cruse, H.: What mechanisms coordinate leg movement in walking arthropods? Trends Neurosci. 13, 15–21 (1990). https://doi.org/10.1016/0166-2236(90)90057-H
- Cruse, H.: The control of the anterior extreme position of the hindleg of a walking insect, Carausius morosus. Physiol. Entomol. 4, 121–124 (1979). https://doi.org/10.1111/j.1365-3032.1979.tb00186.x
- Dallmann, C.J., Hoinville, T., Dürr, V., Schmitz, J.: A load-based mechanism for inter-leg coordination in insects. Proc. R. Soc. B Biol. Sci. 284, 20171755 (2017). https://doi.org/10. 1098/rspb.2017.1755
- Noah, J.A., Quimby, L., Frazier, S.F., Zill, S.N.: Sensing the effect of body load in legs: responses of tibial campaniform sensilla to forces applied to the thorax in freely standing cockroaches. J. Comp. Physiol. A 190, 201–215 (2004). https://doi.org/10.1007/s00359-003-0487-y
- 8. Zill, S., Schmitz, J., Büschges, A.: Load sensing and control of posture and locomotion. Arthropod Struct. Dev. 33, 273–286 (2004). https://doi.org/10.1016/j.asd.2004.05.005

- Noah, A.J., Quimby, L., Frazier, F.S., Zill, S.N.: Force detection in cockroach walking reconsidered: discharges of proximal tibial campaniform sensilla when body load is altered. J. Comp. Physiol. A 187, 769–784 (2001). https://doi.org/10.1007/s00359-001-0247-9
- Kemmerling, S., Varju, D.: Regulation of the body-substrat-distance in the stick insect: responses to sinusoidal stimulation. Biol. Cybern. 39, 129–137 (1981). https://doi.org/10. 1007/BF00336739
- 11. Pearson, K.G.: Central programming and reflex control of walking in the cockroach. J. Exp. Biol. **56**, 173–193 (1972)
- Zill, S.N., Keller, B.R., Duke, E.R.: Sensory signals of unloading in one leg follow stance onset in another leg: transfer of load and emergent coordination in cockroach walking. J. Neurophysiol. 101, 2297–2304 (2009). https://doi.org/10.1152/jn.00056.2009
- 13. Zill, S., Moran, D.T.: The exoskeleton and insect proprioception. I. Responses of tibial campaniform sensilla to external and muscle-generated forces in the American cockroach, Periplaneta Americana. J. Exp. Biol. **91**(1), 1–24 (1981)
- 14. Pringle, J.W.S.: Proprioception in insects: I. A new type of mechanical receptor from the palps of the cockroach. J. Exp. Biol. **15**, 101–113 (1938)
- Dinges, G.F., Chockley, A.S., Bockemühl, T., Ito, K., Blanke, A., Büschges, A.: Location and arrangement of campaniform sensilla in Drosophila melanogaster. J. Comp. Neurol. 529, 905–925 (2021). https://doi.org/10.1002/cne.24987
- Grünert, U., Gnatzy, W.: Campaniform sensilla of Calliphora vicina (Insecta, Diptera).
  Zoomorphology 106, 320–328 (1987). https://doi.org/10.1007/BF00312006
- 17. Merritt, D.J., Murphey, R.K.: Projections of leg proprioceptors within the CNS of the fly Phormia in relation to the generalized insect ganglion. J. Comp. Neurol. **322**, 16–34 (1992). https://doi.org/10.1002/cne.903220103
- 18. Yasuyama, K., Salvaterra, P.M.: Localization of choline acetyltransferase-expressing neurons in Drosophila nervous system. Microsc. Res. Tech. 45, 65–79 (1999). https://doi.org/10.1002/(sici)1097-0029(19990415)45:2%3C65::aid-jemt2%3E3.0.co;2-0
- Delcomyn, F.: Activity and directional sensitivity of leg campaniform sensilla in a stick insect.
  J. Comp. Physiol. A 168, 113–119 (1991). https://doi.org/10.1007/BF00217109
- Hofmann, T., Bässler, U.: Response characteristics of single trochanteral campaniform sensilla in the stick insect, Cuniculina impigra. Physiol. Entomol. 11, 17–21 (1986). https://doi.org/ 10.1111/j.1365-3032.1986.tb00386.x
- 21. Tuthill, J.C., Wilson, R.I.: Mechanosensation and adaptive motor control in insects. Curr. Biol. CB. 26, R1022–R1038 (2016). https://doi.org/10.1016/j.cub.2016.06.070
- Kaliyamoorthy, S., Zill, S.N., Quinn, R.D., Ritzmann, R.E., Choi, J.: finite element analysis of strains in a Blaberus cockroach leg during climbing. In: Proceedings 2001 IEEE/RSJ International Conference on Intelligent Robots and Systems. Expanding the Societal Role of Robotics in the Next Millennium (Cat. No.01CH37180), pp. 833–838. IEEE, Maui, HI, USA (2001). https://doi.org/10.1109/IROS.2001.976272
- 23. Akay, T., Haehn, S., Schmitz, J., Büschges, A.: Signals from load sensors underlie interjoint coordination during stepping movements of the stick insect leg. J. Neurophysiol. **92**, 42–51 (2004). https://doi.org/10.1152/jn.01271.2003
- 24. Marquardt, F.: Beiträge zur Anatomie der Muskulatur und der peripheren Nerven von Carausius Dixippus morosus Br.; Mit 5 Abb. im Text u. Taf (1939)
- Zill, S.N., Schmitz, J., Chaudhry, S., Büschges, A.: Force encoding in stick insect legs delineates a reference frame for motor control. J. Neurophysiol. 108, 1453–1472 (2012). https://doi.org/10.1152/jn.00274.2012
- 26. Hofmann, T., Bässler, U.: Anatomy and physiology of trochanteral campaniform sensilla in the stick insect, Cuniculina impigra. Physiol. Entomol. 7, 413–426 (1982). https://doi.org/10.1111/j.1365-3032.1982.tb00317.x

- 27. Schmitz, J.: Load-compensating reactions in the proximal leg joints of stick insects during standing and walking. J. Exp. Biol. **183**(1), 15–33 (1993)
- Zill, S.N., Neff, D., Chaudhry, S., Exter, A., Schmitz, J., Büschges, A.: Effects of force detecting sense organs on muscle synergies are correlated with their response properties. Arthropod Struct. Dev. 46, 564–578 (2017). https://doi.org/10.1016/j.asd.2017.05.004
- 29. Bässler, U.: A movement generated in the peripheral nervous system: rhythmic flexion by autotomized legs of the stick insect Cuniculina impigra. J. Exp. Biol. 111, 191–199 (1984)
- Schindler: Funktionsmorphologische Untersuchungen zur Autotomie der Stabheuschrecke Carausius morosus Br. (Insecta: Phasmida). Zool. Anz., vol. 203, no. 316 (1979)
- Bordage, E.: XXIII.—On the probable mode of formation of the fusion between the femur and trochanter in Arthropods. J. Nat. History (2009). https://doi.org/10.1080/002229399086 78095
- Soler, C., Daczewska, M., Da Ponte, J.P., Dastugue, B., Jagla, K.: Coordinated development of muscles and tendons of the Drosophila leg. Development 131, 6041 (2004). https://doi. org/10.1242/dev.01527
- 33. Lobato-Rios, V., Ramalingasetty, S.T., Özdil, P.G., Arreguit, J., Ijspeert, A.J., Ramdya, P.: NeuroMechFly, a neuromechanical model of adult Drosophila melanogaster. Nat. Methods. 19, 620–627 (2022). https://doi.org/10.1038/s41592-022-01466-7
- 34. Goldsmith, C.A., Haustein, M., Bockemühl, T., Büschges, A., Szczecinski, N.S.: Analyz-ing 3D limb kinematics of drosophila melanogaster for robotic platform development. In: Hunt, A., et al. (eds.) Biomimetic and Biohybrid Systems, vol. 13548, pp. 111–122. Springer International Publishing, Cham (2022). https://doi.org/10.1007/978-3-031-20470-8 12
- 35. Sink, H.: Muscle Development in Drosophila. Springer, New York, NY (2006). https://doi.org/10.1007/0-387-32963-3
- Dallmann, C.J., Dürr, V., Schmitz, J.: Motor control of an insect leg during level and incline walking. J. Exp. Biol. 222 (2019). https://doi.org/10.1242/jeb.188748
- 37. Akay, T., Ludwar, B.C., Göritz, M.L., Schmitz, J., Büschges, A.: Segment specificity of load signal processing depends on walking direction in the stick insect leg muscle control system. J. Neurosci. 27, 3285–3294 (2007). https://doi.org/10.1523/JNEUROSCI.5202-06.2007
- 38. Zill, S.N., Moran, D.T.: The exoskeleton and insect proprioception: III. Activity of tibial campaniform sensilla during walking in the American cockroach, Periplaneta Americana. J. Exp. Biol. **94**, 57 (1981)
- 39. Goldsmith, C., Szczecinski, N., Quinn, R.: Drosophibot: a fruit fly inspired bio-robot. In: Biomimetic and Biohybrid Systems. Living Machines 2019. LNCS, vol. 11556, pp. 146–157. Springer, Cham (2019). https://doi.org/10.1007/978-3-030-24741-6 13
- Zyhowski, W.P., Zill, S.N., Szczecinski, N.S.: Adaptive load feedback robustly signals force dynamics in robotic model of Carausius morosus stepping. Front. Neurorobot. 17, 1125171 (2023). https://doi.org/10.3389/fnbot.2023.1125171
- 41. Onyx Composite 3D Printing Material. https://markforged.com/materials/plastics/onyx. Accessed 22 Feb 2023
- Haberkorn, A., Gruhn, M., Zill, S.N., Büschges, A.: Identification of the origin of force-feedback signals influencing motor neurons of the thoraco-coxal joint in an insect. J. Comp. Physiol. A 205(2), 253–270 (2019). https://doi.org/10.1007/s00359-019-01334-4
- 43. Delcomyn, F., Nelson, M.E., Cocatre-Zilgien, J.H.: Sense organs of insect legs and the selection of sensors for agile walking robots. Int. J. Robot. Res. 15, 113–127 (1996). https://doi.org/10.1177/027836499601500201
- 44. Bennemann, M., Baumgartner, W., Bräunig, P.-M.: Biomimicry of the adhesive organs of stick insects (Carausius morosus). Fachgruppe Biologie (2015)
- 45. Garcia, M., Kuo, A., Peattie, A., Wang, P., Full, R.J.: Damping and size: insights and biological inspiration. Presented at First International Symposium on Adaptive Motion of Animals and Machines (2000)

- 46. Hooper, S.L., et al.: Neural control of unloaded leg posture and of leg swing in stick insect, cockroach, and mouse differs from that in larger animals. J. Neurosci. **29**, 4109–4119 (2009). https://doi.org/10.1523/JNEUROSCI.5510-08.2009
- Ache, J.M., Matheson, T.: Passive joint forces are tuned to limb use in insects and drive movements without motor activity. Curr. Biol. 23, 1418–1426 (2013). https://doi.org/10.1016/ i.cub.2013.06.024
- 48. Cruse, H., Bartling, C.: Movement of joint angles in the legs of a walking insect, Carausius morosus. J. Insect Physiol. 41, 761–771 (1995). https://doi.org/10.1016/0022-1910(95)000 32-p
- 49. Dickinson, M.H.: Comparison of encoding properties of campaniform sensilla on the fly wing. J. Exp. Biol. **151**, 245 (1990)
- 50. Berendes, V., Zill, S.N., Büschges, A., Bockemühl, T.: Speed-dependent interplay between local pattern-generating activity and sensory signals during walking in Drosophila. J. Exp. Biol. **219**, 3781 (2016). https://doi.org/10.1242/jeb.146720
- 51. Wosnitza, A., Bockemühl, T., Dübbert, M., Scholz, H., Büschges, A.: Inter-leg coordination in the control of walking speed in Drosophila. J. Exp. Biol. **216**, 480 (2013). https://doi.org/10.1242/jeb.078139